the yield of the latter might be improved by reverse addition.

Acknowledgment. It is a pleasure to acknowledge financial support of this work by the National Science Foundation and the Materials Science Center of Cornell University. We thank the M and T Chemical Co. for samples of organotin compounds.

Registry No. $(ClZn)_2Fe(CO)_4$, 65991-65-3; $(Ph_3Sn)_2Fe(CO)_4$, 21868-08-6; $[n\text{-}Bu_2SnFe(CO)_4]_2$, 15613-38-4; $(n\text{-}Bu_3Sn)_2Fe(CO)_4$, 61788-09-8; $(ClHg)_2Fe(CO)_4$, 15281-84-2; Ph_3SnCl, 639-58-7; $n\text{-}Bu_2SnCl_2$, 683-18-1; $n\text{-}Bu_3SnCl$, 1461-22-9.

References and Notes

(1) E. H. Brooks and R. J. Cross, *Organomet. Chem. Rev., Sect A*, **6**, 227 (1970), and references cited therein.
(2) J. E. Ellis, *J. Organomet. Chem.*, **86**, 1 (1975), and references cited therein.
(3) (a) J. P. Collman, *Acc. Chem. Res.*, **8**, 342 (1975); (b) R. G. Komoto, Ph.D. Thesis, Stanford University, 1974.
(4) S. E. Hayes, Ph.D. Thesis, Cornell University, 1974.
(5) R. C. Winterton, Ph.D. Thesis, Cornell University, 1977.
(6) J. St. Denis, W. Butler, M. D. Glick, and J. P. Oliver, *J. Am. Chem. Soc.*, **96**, 5427 (1974).
(7) D. E. Crotty, E. R. Corey, T. J. Anderson, M. D. Glick, and J. P. Oliver, *Inorg. Chem.*, **16**, 920 (1977).
(8) D. E. Crotty, T. J. Anderson, M. D. Glick, and J. P. Oliver, *Inorg. Chem.*, **16**, 2346 (1977).
(9) D. Crotty and J. P. Oliver, *Inorg. Chem.*, **16**, 2501 (1977).
(10) J. M. Burlitch and T. W. Theyson, *J. Chem. Soc., Dalton Trans.*, 828 (1974).
(11) H. W. Sternberg, I. Wender, and M. Orchin, *Anal. Chem.*, **24**, 174 (1952).
(12) M. Orchin and I. Wender, *Anal. Chem.*, **21**, 875 (1949).
(13) H. Gilman and W. B. King, *J. Am. Chem. Soc.*, **51**, 1213 (1929).
(14) H. Hock and H. Stuhlman, *Chem. Ber.*, **61**, 2097 (1928).
(15) F. Hein and W. Jehn, *Justus Liebigs Ann. Chem.*, **684**, 4 (1965).
(16) J. D. Cotton, S. A. R. Knox, I. Paul, and F. G. A. Stone, *J. Chem. Soc. A*, 264 (1967).
(17) J. M. Burlitch and A. Ferrari, *Inorg. Chem.*, **9**, 563 (1970).
(18) T. Tanako and Y. Sasaki, *Bull. Chem. Soc. Jpn.*, **44**, 431 (1971).
(19) F. Galembeck and P. Krumholz, *J. Am. Chem. Soc.*, **93**, 1909 (1971).
(20) J. Dalton, I. Paul, and F. G. A. Stone, *J. Chem. Soc. A*, 1215 (1968).
(21) A. A. Chalmers, J. Lewis, and S. B. Wild, *J. Chem. Soc. A*, 1013 (1968).
(22) H. W. Baird and L. F. Dahl, *J. Organomet. Chem.*, **7**, 503 (1967).
(23) R. A. Burnham, M. A. Lyle and S. R. Stobart, *J. Organomet. Chem.*, **125**, 179 (1977).

Contribution from the Department of Chemistry and the Molecular Structure Center, Indiana University, Bloomington, Indiana 47401

π Complexes of Nickel(0) and Ketones. Mechanism of Formation and the Crystal Structure of (Benzophenone)bis(triethylphosphine)nickel

T. T. Tsou, J. C. Huffman, and J. K. Kochi*

Received April 2, 1979

Transition metals form complexes with a variety of ligands containing a carbonyl functionality. Of these, the β-diketonate complexes, which are among the most common, derive their stability from the formation of chelates with the bidentate ligand. Some simple carbonyl compounds also form stable metal complexes. Thus, monofunctional ketones such as acetone, chloroacetone, and butanone[1] and aldehydes such as acetaldehyde, propionaldehyde, and benzaldehyde,[2] as well as esters such as methyl formate and ethyl acetate,[3] all form stable complexes, especially with divalent transition-metal ions. The carbonyl group in these complexes is usually coordinated through an oxygen atom by σ bonding, and metal ions surrounded by six oxygen atoms in an octahedral array have been described.[4]

Although rare, there are some examples in which the carbonyl group is π bonded to the metal. Thus, hexafluoroacetone forms a π complex with nickel(0) in which structural data clearly indicate a sidewise coordination of the carbonyl group.[5] Benzaldehyde and benzophenone also form stable red complexes with (triphenylphosphine)nickel(0).[6] More recently, a zerovalent nickel complex of *tert*-butyl isocyanide was reported to afford stable complexes with carbonyl compounds containing electron-withdrawing substituents.[7] The latter suggests that back-bonding is an important factor in the formation of π complexes of carbonyl compounds with metals, particularly those in low formal oxidation states.

In this study we wish to employ polar substituents on the aromatic ring of benzophenone to probe the mechanism of the formation of π complexes of nickel(0). The parent member of the series has been isolated as a red crystalline compound with composition $(Ph_2C{=}O)Ni(PEt_3)_2$. The X-ray crystal structure of the π-bonded carbonyl group is compared with the π bonding of other unsaturated ligands.

Results and Discussion

The triethylphosphine complex of nickel(0) is isolated as a colorless crystalline solid of composition $Ni(PEt_3)_4$. The complex is labile, and in organic solvents such as tetrahydrofuran (THF), benzene, or hexane it readily dissociates to coordinatively unsaturated species (eq 1). For example,

$$Ni(PEt_3)_4 \underset{-PEt_3}{\overset{K_1}{\rightleftharpoons}} Ni(PEt_3)_3 \underset{-PEt_3}{\overset{K_2}{\rightleftharpoons}} Ni(PEt_3)_2 \quad (1)$$

K_1 and K_2 are 1.0×10^{-2} and $<10^{-6}$, respectively, in THF solution. The red color of the solution is associated with $Ni(PEt_3)_3$ absorbing at 500 nm (ϵ 3900).[8]

Product and Stoichiometry. Upon the addition of 1 equiv of benzophenone, the band at 500 nm disappeared with the concomitant growth of a new band at 330 nm. A red crystalline product I (eq 2) could be isolated from this solution.

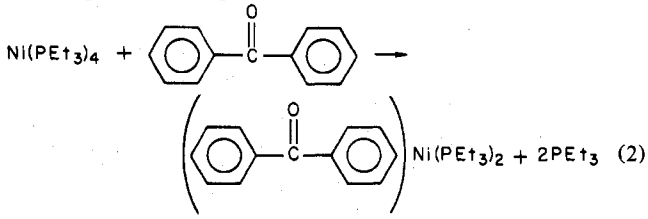

I

A similar reaction occurred with acetophenone, but we were unable to isolate a crystalline product. The addition of acetone or methyl benzoate to the red solution under the same conditions did not affect either the position, shape, or intensity of the absorption band at 500 nm. The formation constants with these carbonyl compounds are apparently small, since the red color of $Ni(PEt_3)_3$ is not visible in a solution of $Ni(PEt_3)_4$ in the neat solvent (e.g., acetone). Qualitatively, weak π complexes with dimethylformamide (e.g., eq 3) are also indicated by solutions showing a much less intense absorbance at 500 nm compared to that observed in noncoordinating solvents such as THF, benzene, or hexane.

$$Ni(PEt_3)_4 + (CH_3)_2NHC{=}O \rightleftharpoons [(CH_3)_2NHC{=}O]Ni(PEt_3)_2 + 2PEt_3 \quad (3)$$

Upon coordination to nickel(0), the infrared stretching frequencies of the carbonyl groups of benzophenone and acetophenone at 1680 and 1690 cm^{-1}, respectively, disappeared.[9] The complexed benzophenone can be displaced from nickel(0) simply by bubbling carbon monoxide through the solution. The substitution reaction proceeds quantitatively according to eq 4, as indicated by the complete reappearance of the carbonyl frequency of free benzophenone as well as the growth of the characteristic bands at 1995 and 1935 cm^{-1} for $Ni(CO)_2(PEt_3)_2$.[10] The red complex of (benzophenone)bis(triethylphosphine)nickel is air sensitive and melts between

$$(PhCOPh)Ni(PEt_3)_2 + 2CO \rightarrow PhCOPh + Ni(CO)_2(PEt_3)_2 \quad (4)$$

0020-1669/79/1318-2311$01.00/0

Table I. Phosphine Dependence of the Observed Second-Order Rate Constant for π Nickel(0) Formation[a]

added $[PEt_3]$, M	k_{obsd}, M^{-1} s^{-1}	added $[PEt_3]$, M	k_{obsd}, M^{-1} s^{-1}
0	21.3	6.75×10^{-3}	8.50
2.25×10^{-3}	13.9	9.00×10^{-3}	7.28
4.50×10^{-3}	11.1		

[a] In toluene solution containing $[Ni(PEt_3)_4] = 5 \times 10^{-4}$ M and [*p*-(*N*,*N*-dimethylamino)benzophenone] = 5×10^{-3} M at 25 °C.

70 and 78 °C to afford a red liquid. The proton NMR spectrum at 60 MHz in benzene-d_6 consists of partially resolved multiplet resonances for both the ethyl (δ 0.3–1.7) and phenyl (δ 7.18 and 8.18) groups, but the ^{31}P NMR spectrum shows two sharp singlets at 19.37 and 19.51 ppm downfield from phosphoric acid, consistent with the structure described below.

Kinetics and Mechanism of π-Complex Formation. The rate of the reaction between $Ni(PEt_3)_4$ and benzophenone was followed spectrophotometrically by monitoring the disappearance of the 500 nm band. The formation of the π nickel(0) complex obeys apparent second-order kinetics, being first order in $Ni(PEt_3)_3$ and benzophenone according to eq 5,

$$-d[NiL_3]/dt = k_{obsd}[PhCOPh][NiL_3] \quad (5)$$

where L = PEt_3. The observed second-order rate constant, however, is diminished by added triethylphosphine as listed in Table I. Quantitatively the inverse phosphine dependence of the observed rate constant is given by eq 6 as illustrated

$$\frac{1}{k_{obsd}} = \frac{1}{k}\left\{1 + \frac{[PEt_3]}{K}\right\} \quad (6)$$

in Figure 1. The value of the phosphine-independent rate constant $k = 22.2$ M^{-1} s^{-1} obtained from the intercept affords a value of $K = 4.2 \times 10^{-3}$ M derived from the slope.

Such a relationship for the phosphine dependence would obtain if the three-coordinate nickel(0) were the species directly involved in π-complex formation (Scheme I).

Scheme I

$$NiL_4 \overset{K_1}{\rightleftharpoons} NiL_3 + L \quad (7)$$

$$NiL_3 + Ar_2C{=}O \xrightarrow{k_2} (Ar_2C{=}O)NiL_2 + L \quad (8)$$

The kinetics of π-complex formation according to the mechanism in Scheme I is given by the rate equation in eq 9, if the phosphine dissociation in eq 7 is fast, where $k_{obsd} =$

$$-\frac{d[NiL_3]}{dt} = \frac{K_1k_2}{K_1 + [L]}[Ar_2CO][NiL_3] \quad (9)$$

$K_1k_2/\{K_1 + [L]\}$, the inverse of which is equivalent to eq 6, where $k = k_2$ and $K = K_1$. Indeed, $K_1 = 4.2 \times 10^{-3}$ M, independently evaluated by a spectral technique (see eq 1), is the same as that determined kinetically from eq 6.

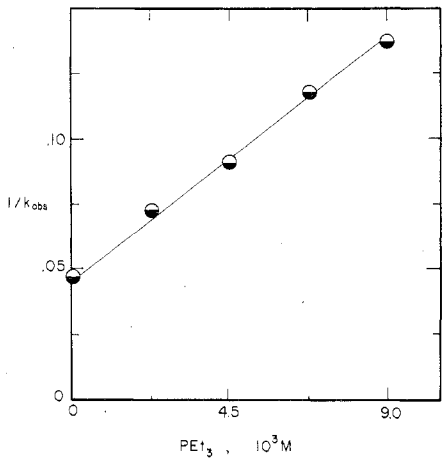

Figure 1. Phosphine dependence on the rate of π-complex formation between $Ni(PEt_3)_4$ and *p*-(*N*,*N*-dimethylamino)benzophenone in toluene at 25 °C.

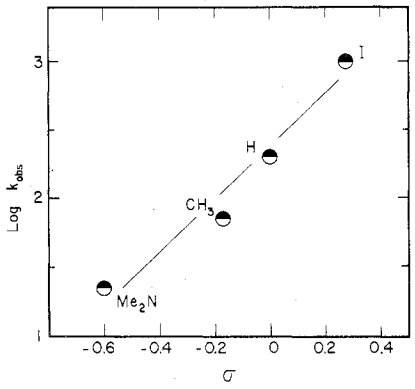

Figure 2. Hammett correlation of the rate of π-complex formation from $Ni(PEt_3)_4$ and substituted benzophenones.

The effect of polar, nuclear substituents on the rate of π-complex formation was examined under standard conditions by employing the ketone in excess to approximate zero-order kinetics. The pseudo-first-order rate constant k_1 obtained in this manner shows a first-order dependence on the concentration of benzophenone as listed in Table II. The Hammett correlation of the second-order rate constants for substituted benzophenones with $\rho = +2.0$ is illustrated in Figure 2. These rate constants (log k_{obsd}) are also linearly related to the reduction potentials[11] of the corresponding substituted benzophenones shown in Figure 3. In both cases, the rate of π-complex formation is accelerated by relatively electron-deficient benzophenones and retarded by electron-rich benzophenones.

Table II. Substituent Effects on the Kinetics of the Formation of Benzophenone π Complexes with Nickel(0)[a]

σ	R	$[4\text{-}RC_6H_4\text{-}COC_6H_5]$, M	$10^4[Ni(PEt_3)_4]$, M	solvent	k_1, s^{-1}	k_{obsd},[b] M^{-1} s^{-1}	E_0,[c] V
−0.60	Me_2N	5.0×10^{-3}	5.0	benzene	0.11	2.2 × 10 (1.34)	−1.90
−0.17	CH_3	5.0×10^{-3}	5.0	benzene	0.35	7.0 × 10 (1.84)	−1.76
0	H	5.0×10^{-3}	5.0	benzene	1.2	2.4×10^2 (2.38)	−1.68
0	H	1.0×10^{-2}	5.0	benzene	1.8	1.8×10^2 (2.25)	−1.68
0	H	1.5×10^{-2}	5.0	benzene	3.2	2.1×10^2 (2.32)	−1.68
0.28	I	5.0×10^{-3}	5.0	benzene	4.9[d]	9.9×10^2(2.99)	−1.60[e]
0.82	Me_3N^+	5.0×10^{-3}	5.0	THF	3.6 × 10	7.3×10^3 (3.86)	−1.42
−0.60	Me_2N	4.2×10^{-4}	4.2	hexane		3.9 × 10 (1.59)	−1.90
0	H	4.2×10^{-4}	4.2	hexane		4.3×10^2 (2.63)	−1.68

[a] In benzene solutions at 25 °C, as described in the text. [b] Logarithms in parentheses. [c] Reduction potentials of benzophenone in DMF solution are from ref 11. [d] A subsequent reaction affords the oxidative adduct $PhCOC_6H_4NiI(PEt_3)_2$. [e] Interpolated value obtained from Figure 3.

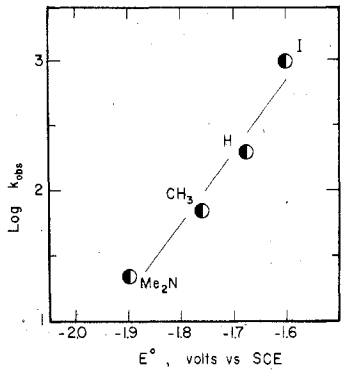

Figure 3. Relationship between the electrochemical reduction potentials of substituted benzophenones and the rates of π-complex formation from $Ni(PEt_3)_4$.

The linear correlation of the rates with the reduction potentials of the benzophenone as well as the positive Hammett ρ value indicates that the electron density flows from the nickel center to the incipient benzophenone ligand in the transition state for π-complex formation. However, electron transfer is not complete, since the well-characterized ESR signals of neither the paramagnetic nickel(I) species[12] nor the benzophenone ketyl[13] can be observed. Furthermore, when the benzophenone ketyl (prepared independently) was added to solutions of either nickel(I) or nickel(II), the reverse process involving electron transfer *from* the ketyl obtained (eq 10 and 11). In both cases, the formation of the (benzophenone)-

$$K^+(PhCOPh)^-\cdot + BrNi(PEt_3)_3 \xrightarrow[-KBr]{} (PhCOPh)Ni(PEt_3)_2 + PEt_3 \quad (10)$$

$$2K^+(PhCOPh)^-\cdot + Br_2Ni(PEt_3)_2 \xrightarrow[-2KBr]{} (PhCOPh)Ni(PEt_3)_2 + PhCOPh \quad (11)$$

nickel(0) complex was readily observed by its characteristic visible absorption, proton NMR, and IR spectra.

The substituent effects on the rates of π-complex formation suggest several mechanisms. [The inverse phosphine dependence indicates that the fully coordinated tetrakis(triethylphosphine)nickel is not directly involved.[14]] The rate-limiting step presented above in Scheme I is an associative process in which the π complex is formed by a direct ligand displacement of phosphine from the three-coordinate $Ni(PEt_3)_3$ by benzophenone. An alternative dissociative process is included in Scheme II, in which the loss of phosphine from the four-coordinate benzophenone adduct in eq 14 represents the important activation process (Scheme II).

Scheme II

$$NiL_4 \overset{K_1}{\rightleftharpoons} NiL_3 + L \quad (12)$$

$$NiL_3 + Ar_2C{=}O \overset{K}{\rightleftharpoons} (Ar_2C{=}O)NiL_3 \quad (13)$$

$$(Ar_2C{=}O)NiL_3 \xrightarrow{k_2} (Ar_2C{=}O)NiL_2 + L \quad (14)$$

However, without the actual detection of $(Ar_2C{=}O)Ni(PEt_3)_3$ as an intermediate, the distinction between the mechanisms in Schemes I and II is difficult to make rigorously. The solvent dependence of the rate of π-complex formation in Table III is rather small, but suggests a slightly decreasing order: hexane > toluene > THF.

Crystal Structure of (Benzophenone)bis(triethylphosphine)nickel. To avoid decomposition, a crystal of I was placed in a gaseous stream of cold nitrogen on the goniostat and maintained at −145 °C throughout the characterization and data collection. The X-ray structure shown in Figure 4 indicates that the carbonyl group bonded to nickel has a trigonal-planar configuration, with bond distances and angles listed in Tables IV and V, respectively. The nonbonded contact distances are normal, showing the data crystal to be composed of an array of neutral molecules.

Table III. Solvent Dependence of the Rate of π-Complex Formation[a]

solvent	k_{obsd}, M^{-1} s^{-1}	solvent	k_{obsd}, M^{-1} s^{-1}
hexane	49	THF	11
toluene	22		

[a] For *p*-(*N*,*N*-dimethylamino)benzophenone at 25 °C. [ArCOPh] = 5.0 × 10^{-3} M and [$Ni(PEt_3)_4$] = 5.0 × 10^{-4} M.

Table IV. Bond Distances (Å) for $Ni[(C_6H_5)_2CO][P(C_2H_5)_3]_2$

A	B	dist	A	B	dist
Ni(1)	P(1)	2.136 (1)	C(9)	H(6)	0.985 (27)
Ni(1)	P(2)	2.190 (1)	C(10)	H(7)	1.006 (36)
Ni(1)	O(1)	1.849 (2)	C(11)	H(8)	1.016 (45)
Ni(1)	C(1)	1.974 (3)	C(12)	H(9)	0.894 (41)
P(1)	C(14)	1.832 (4)	C(13)	H(10)	0.963 (59)
P(1)	C(16)	1.831 (4)	C(14)	H(11)	1.029 (46)
P(1)	C(18)	1.829 (4)	C(14)	H(12)	0.963 (44)
P(2)	C(20)	1.837 (4)	C(15)	H(13)	1.048 (53)
P(2)	C(22)	1.834 (4)	C(15)	H(14)	0.876 (50)
P(2)	C(24)	1.830 (4)	C(15)	H(15)	0.827 (64)
O(1)	C(1)	1.335 (4)	C(16)	H(16)	0.989 (44)
C(1)	C(2)	1.509 (5)	C(16)	H(17)	0.978 (43)
C(1)	C(8)	1.491 (5)	C(17)	H(18)	0.975 (53)
C(2)	C(3)	1.397 (5)	C(17)	H(19)	0.892 (43)
C(2)	C(7)	1.390 (5)	C(17)	H(20)	1.175 (52)
C(3)	C(4)	1.389 (5)	C(18)	H(21)	0.924 (44)
C(4)	C(5)	1.377 (6)	C(18)	H(22)	0.911 (48)
C(5)	C(6)	1.399 (5)	C(19)	H(23)	0.917 (43)
C(6)	C(7)	1.384 (5)	C(19)	H(24)	0.867 (39)
C(8)	C(9)	1.392 (5)	C(19)	H(25)	1.015 (66)
C(8)	C(13)	1.406 (5)	C(20)	H(26)	0.921 (47)
C(9)	C(10)	1.381 (5)	C(20)	H(27)	1.051 (43)
C(10)	C(11)	1.390 (6)	C(21)	H(28)	1.058 (59)
C(11)	C(12)	1.373 (7)	C(21)	H(29)	0.904 (51)
C(12)	C(13)	1.388 (6)	C(21)	H(30)	1.010 (53)
C(14)	C(15)	1.512 (6)	C(22)	H(31)	0.931 (51)
C(16)	C(17)	1.516 (6)	C(22)	H(32)	0.901 (55)
C(18)	C(19)	1.518 (5)	C(23)	H(33)	0.795 (50)
C(20)	C(21)	1.526 (6)	C(23)	H(34)	0.963 (46)
C(22)	C(23)	1.519 (5)	C(23)	H(35)	0.970 (73)
C(24)	C(25)	1.517 (5)	C(24)	H(36)	0.744 (55)
C(3)	H(1)	0.923 (40)	C(24)	H(37)	0.996 (37)
C(4)	H(2)	1.031 (30)	C(25)	H(38)	0.844 (51)
C(5)	H(3)	0.978 (42)	C(25)	H(39)	0.923 (33)
C(6)	H(4)	0.926 (49)	C(25)	H(40)	0.949 (40)
C(7)	H(5)	0.822 (41)			

The carbonyl group in I is associated with nickel by a sideways attachment to form a rigid O–Ni–C ring. The length of the C=O bond of 1.335 (4) Å is approximately 0.1 Å longer than that (1.23 Å) of the free benzophenone structure.[15] The same bond extension is observed in the (hexafluoroacetone)nickel(0) complex in which the C=O bond length is 1.32 (2) Å. The lengthening of the C=O bond can be interpreted in terms of the Dewar–Chatt–Duncanson model of π bonding[16] as arising from a back-donation from a metal d orbital into the antibonding π^* orbital of the carbonyl group. Such a back-bonding is expected not only to weaken the C=O bond but also to lead to a change of the configuration of the carbonyl carbon from an idealized sp^2 hybridized state toward an sp^3 state upon coordination. Indeed, such an expansion of the internal angle C(2)–C(1)–C(8) from 122° in the free ligand to 119.3 (3)° upon coordination is observed, although of limited magnitude.

The structural parameters involved in π bonding of carbonyl ligands to nickel are compared in Table VI. The coordination of the carbonyl group to nickel is not symmetrical in I, the

Table V. Bond Angles (deg) for $Ni[(C_6H_5)_2CO][P(C_2H_5)_3]_2$

A	B	C	angle	A	B	C	angle
P(1)	Ni(1)	P(2)	106.0 (0)	P(1)	C(14)	H(11)	105.6 (27)
P(1)	Ni(1)	O(1)	153.4 (1)	P(1)	C(14)	H(12)	113.2 (25)
P(1)	Ni(1)	C(1)	112.8 (1)	C(15)	C(14)	H(11)	110.2 (24)
P(2)	Ni(1)	O(1)	100.6 (1)	C(15)	C(14)	H(12)	112.8 (26)
P(2)	Ni(1)	C(1)	141.2 (1)	H(11)	C(14)	H(12)	101.1 (36)
O(1)	Ni(1)	C(1)	40.7 (1)	C(14)	C(15)	H(13)	110.3 (28)
Ni(1)	P(1)	C(14)	115.2 (1)	C(14)	C(15)	H(14)	116.3 (30)
Ni(1)	P(1)	C(16)	113.8 (1)	C(14)	C(15)	H(15)	113.9 (38)
Ni(1)	P(1)	C(18)	117.0 (1)	H(13)	C(15)	H(14)	111.9 (39)
C(14)	P(1)	C(16)	102.7 (2)	H(13)	C(15)	H(15)	98.9 (48)
C(14)	P(1)	C(18)	102.9 (2)	H(14)	C(15)	H(15)	104.2 (47)
C(16)	P(1)	C(18)	103.4 (2)	P(1)	C(16)	H(16)	104.4 (21)
Ni(1)	P(2)	C(20)	117.9 (1)	P(1)	C(16)	H(17)	103.5 (24)
Ni(1)	P(2)	C(22)	108.3 (1)	C(17)	C(16)	H(16)	109.2 (24)
Ni(1)	P(2)	C(24)	120.7 (1)	C(17)	C(16)	H(17)	114.7 (24)
C(20)	P(2)	C(22)	103.3 (2)	H(16)	C(16)	H(17)	111.3 (35)
C(20)	P(2)	C(24)	100.8 (2)	C(16)	C(17)	H(18)	107.1 (31)
C(22)	P(2)	C(24)	103.7 (2)	C(16)	C(17)	H(19)	108.0 (30)
Ni(1)	O(1)	C(1)	74.7 (2)	C(16)	C(17)	H(20)	111.2 (24)
Ni(1)	C(1)	O(1)	64.6 (2)	H(18)	C(17)	H(19)	121.5 (42)
Ni(1)	C(1)	C(2)	116.3 (2)	H(18)	C(17)	H(20)	100.7 (39)
Ni(1)	C(1)	C(8)	110.7 (2)	H(19)	C(17)	H(20)	108.1 (35)
O(1)	C(1)	C(2)	116.0 (3)	P(1)	C(18)	H(21)	107.0 (28)
O(1)	C(1)	C(8)	117.8 (3)	P(1)	C(18)	H(22)	104.3 (31)
C(2)	C(1)	C(8)	119.3 (3)	C(19)	C(18)	H(21)	111.3 (29)
C(1)	C(2)	C(3)	119.5 (3)	C(19)	C(18)	H(22)	109.1 (28)
C(1)	C(2)	C(7)	123.2 (3)	H(21)	C(18)	H(22)	107.2 (39)
C(3)	C(2)	C(7)	117.0 (3)	C(18)	C(19)	H(23)	105.7 (25)
C(2)	C(3)	C(4)	121.8 (3)	C(18)	C(19)	H(24)	109.1 (27)
C(3)	C(4)	C(5)	120.0 (3)	C(18)	C(19)	H(25)	119.7 (34)
C(4)	C(5)	C(6)	119.4 (3)	H(23)	C(19)	H(24)	115.7 (36)
C(5)	C(6)	C(7)	119.7 (3)	H(23)	C(19)	H(25)	95.5 (43)
C(2)	C(7)	C(6)	122.0 (3)	H(24)	C(19)	H(25)	110.8 (40)
C(1)	C(8)	C(9)	123.9 (3)	P(2)	C(20)	H(26)	111.9 (31)
C(1)	C(8)	C(13)	118.9 (3)	P(2)	C(20)	H(27)	108.3 (22)
C(9)	C(8)	C(13)	117.2 (3)	C(21)	C(20)	H(26)	105.5 (30)
C(8)	C(9)	C(10)	121.4 (3)	C(21)	C(20)	H(27)	110.0 (23)
C(9)	C(10)	C(11)	120.5 (4)	H(26)	C(20)	H(27)	106.6 (37)
C(10)	C(11)	C(12)	119.2 (4)	C(20)	C(21)	H(28)	109.6 (31)
C(11)	C(12)	C(13)	120.5 (4)	C(20)	C(21)	H(29)	113.3 (32)
C(8)	C(13)	C(12)	121.2 (4)	C(20)	C(21)	H(30)	116.0 (32)
P(1)	C(14)	C(15)	112.9 (3)	H(28)	C(21)	H(29)	105.7 (44)
P(1)	C(16)	C(17)	113.2 (3)	H(28)	C(21)	H(30)	107.7 (44)
P(1)	C(18)	C(19)	117.3 (3)	H(29)	C(21)	H(30)	103.8 (42)
P(2)	C(20)	C(21)	114.2 (3)	P(2)	C(22)	H(31)	108.3 (28)
P(2)	C(22)	C(23)	118.3 (3)	P(2)	C(22)	H(32)	108.3 (36)
P(2)	C(24)	C(25)	113.9 (3)	C(23)	C(22)	H(31)	108.3 (30)
C(2)	C(3)	H(1)	119.6 (23)	C(23)	C(22)	H(32)	108.6 (36)
C(4)	C(3)	H(1)	118.1 (23)	H(31)	C(22)	H(32)	104.1 (45)
C(3)	C(4)	H(2)	117.7 (18)	C(22)	C(23)	H(33)	113.3 (36)
C(5)	C(4)	H(2)	122.1 (18)	C(22)	C(23)	H(34)	107.4 (28)
C(4)	C(5)	H(3)	120.3 (25)	C(22)	C(23)	H(35)	104.6 (45)
C(6)	C(5)	H(3)	120.0 (25)	H(33)	C(23)	H(34)	108.4 (43)
C(5)	C(6)	H(4)	125.9 (28)	H(33)	C(23)	H(35)	120.1 (52)
C(7)	C(6)	H(4)	114.3 (28)	H(34)	C(23)	H(35)	102.0 (48)
C(2)	C(7)	H(5)	120.9 (30)	P(2)	C(24)	H(36)	105.1 (43)
C(6)	C(7)	H(5)	117.1 (30)	P(2)	C(24)	H(37)	104.4 (22)
C(8)	C(9)	H(6)	115.3 (17)	C(25)	C(24)	H(36)	106.7 (42)
C(10)	C(9)	H(6)	123.3 (17)	C(25)	C(24)	H(37)	115.6 (20)
C(9)	C(10)	H(7)	116.0 (19)	H(36)	C(24)	H(37)	110.8 (45)
C(11)	C(10)	H(7)	123.4 (19)	C(24)	C(25)	H(38)	110.4 (31)
C(10)	C(11)	H(8)	125.4 (27)	C(24)	C(25)	H(39)	111.4 (21)
C(12)	C(11)	H(8)	115.0 (27)	C(24)	C(25)	H(40)	104.8 (22)
C(11)	C(12)	H(9)	119.1 (28)	H(38)	C(25)	H(39)	108.2 (37)
C(13)	C(12)	H(9)	120.4 (28)	H(38)	C(25)	H(40)	113.3 (41)
C(8)	C(13)	H(10)	116.7 (29)	H(39)	C(25)	H(40)	108.8 (31)
C(12)	C(13)	H(10)	122.0 (29)				

Ni–O distance of 1.849 (2) Å being 0.125 Å shorter than the Ni–C distance of 1.974 (3) Å. This asymmetry is also reflected in the bond angles. Thus, the O(1)–Ni(1)–P(2) angle of 100.6 (1)° is smaller than the C(1)–Ni(1)–P(1) angle of 112.8 (1)° by 12.2°. It should be noted that in the (hexafluoroacetone)bis(triphenylphosphine)nickel complex, the Ni–C and Ni–O distances are approximately equal, being 1.89 (2) and 1.87 (1) Å, respectively. The two nickel–phosphine distances are also significantly different in I. The bond which is trans to carbon is 2.190 (1) Å, which is 0.054 Å longer than the Ni–P bond trans to oxygen of 2.136 (1) Å. A similar phenomenon has been observed in several π complexes in which the two ends of the unsaturated coordinated ligands are at different distances from the metal. For example, in $Ni[P(O\text{-}o\text{-}tol)_3]_2[H_2C{=}CH(CN)]$ (II), the cyano end of the olefin is significantly closer to the metal, and the trans phosphite

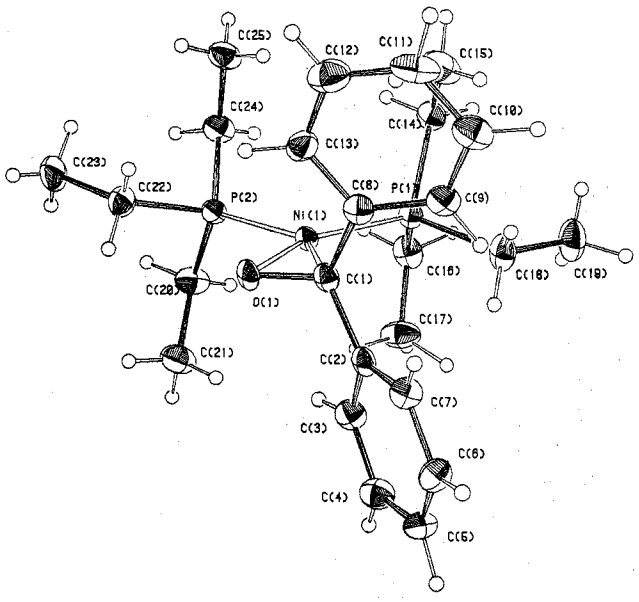

Figure 4. ORTEP drawing of the molecule $Ni[(C_6H_5)_2CO][P(C_2H_5)_3]_2$. All thermal ellipsoids are drawn at the 50% probability level, and hydrogens have been given an artificial B_{iso} = 0.5 Å^2 for artistic purposes. The drawing also shows the numbering scheme used in the tables.

Table VI. Comparative Structural Data of π-Bonded Carbonyl Complexes of Nickel(0)

bond dist or angle	$(Ph_3P)_2Ni(C(=O)(CF_3)CF_3)$ [a]	$(Et_3P)_2Ni(C(=O)(Ph)Ph)$ [a]	$(Cy_3P)_2Ni(C(=O)C)$ [b]
C=O, Å	1.32 (2)	1.335 (4)	1.22 (2)
Δ(C=O),[c] Å	0.09	0.10	0.06
Ni-C, Å	1.89 (2)	1.974 (3)	1.84 (2)
Ni-O, Å	1.87 (1)	1.849 (2)	1.99 (2)
Ni-P(trans to C), Å	2.249 (7)	2.190 (1)	
Ni-P(trans to O), Å	2.175 (6)	2.136 (1)	
$\angle$O-Ni-C, deg	41.3 (7)	40.7 (1)	37
θ,[d] deg	6.9	3.3	
β,[e] deg	48	63.4	

[a] From ref 5. [b] Tricyclohexylphosphine complex taken from ref 17. [c] Extension of the C=O bond length upon coordination. [d] Dihedral angle between the planes Ni-P(1)-P(2) and Ni-C(1)-O(1) (represents a measure of the twist of the unsaturated coordinated ligand toward the coordination plane). [e] Angle between the C=O bond and the normal to the substituent plane of the carbonyl group (represents a measure of the nonplanarity of the bonded carbonyl group).

ligand is closer to the metal than is the cis phosphite.[18] In $(t\text{-BuNC})_2Ni[t\text{-BuN=C=C(CN)}_2]$ (III), the more elec-

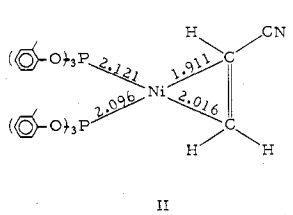

II

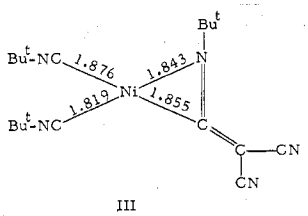

III

tronegative nitrogen is closer to the metal, and the ligand trans to the nitrogen is also closer to the metal.[19] Likewise, the phosphine ligand trans to the more electronegative oxygen in (hexafluoroacetone)bis(triphenylphosphine)nickel is significantly closer to the metal than the other phosphine.

Such a trans influence in π complexes of electron-rich zerovalent nickel with unsaturated C=C ligands derives from an important contribution from π back-bonding. Thus, the presence of an electron-withdrawing substituent, which lowers the energy of the antibonding π^* orbital of the unsaturated ligand, favors the formation of the π complex. Replacement of a trigonal carbon with a more electronegative atom has an effect similar to the introduction of an electron-withdrawing substituent.[20] With either type of unsaturated ligand, the more electron-deficient terminus will have a stronger π-accepting capability and lead to shorter bonds with both trans ligands.

Table VII. Dihedral Angles (θ) for Trigonally Coordinated Nickel(0) Complexes with π Ligands

π complex	θ, deg	ref
$(Ph_3P)Ni(CH_2{=}N(CH_3)_2)Cl$	3.8 (2)	21
$(Ph_3P)_2Ni(CH_2{=}CH_2)$	5	22
$[(o\text{-CH}_3C_6H_4O)_3P]_2Ni(CH_2{=}CH_2)$	6.6	18
$[(C_6H_{11})_2PCH_2]_2Ni(Me_2C{=}CMe_2)$	16.5	23
$(t\text{-BuNC})_2Ni(TCNE)$	23.9 (2)	24
$[(o\text{-CH}_3C_6H_4O)_3P]_2Ni(CH_2{=}CHCN)$	3.9 (1)	18
$(t\text{-BuNC})_2Ni[t\text{-Bu-N=C=C(CN)}_2]$	7.9 (3)	19

Coordination of benzophenone to nickel(0) also destroys the coplanarity of the carbonyl group in the free ligand. The two phenyl groups in I are bent away from the metal, the extent of bending indicated by a β in Table VI of 63.4° rather than 90° for the angle subtended by the C=O bond and the normal to the C(2)-C(1)-C(8) plane. The bending is smaller than that observed in the hexafluoroacetone complex in which β is 48°, presumably due to restoring forces which tend to preserve the π conjugation between the carbonyl group and the phenyl rings. Moreover, the difference in β is not accounted for by steric effects since the phenyl group is expected to be bulkier than the trifluoromethyl group.

The carbonyl group in the (benzophenone)nickel(0) complex is also twisted out of the coordination plane of nickel which is common in trigonal-planar d^{10} structures. The angle θ between the plane defined by P(1)-Ni-P(2) and O(1)-Ni-C(1) is 3.3° which is small compared to that of other trigonally coordinated nickel(0) complexes containing π-bonded ligands listed in Table VII. The carbon atom is about 0.024 Å above the plane defined by P(1)-Ni-P(2), and the oxygen atom is 0.051 Å below this plane. No satisfactory explanation is available to account for this distortion from planarity in these systems.

Experimental Section

Materials. Tetrakis(triethylphosphine)nickel(0) was prepared according to the literature method.[25] The benzophenones either were available commercially or were prepared according to standard literature procedures. All operations involving air-sensitive nickel complexes were carried out with Schlenk flasks under an argon atmosphere by using standard bench-top techniques. Solvents used were all redistilled from sodium/benzophenone under argon first and then redistilled from $Ni(PEt_3)_4$ under argon prior to use.

Interaction of Benzophenone with $Ni(PEt_3)_4$. The infrared study of the interaction between benzophenone and $Ni(PEt_3)_4$ was carried out in 0.05 M THF solutions. Spectra were recorded on a Perkin-Elmer 467 spectrometer. After addition of gaseous carbon monoxide to the reaction mixture, the red color disappeared, and the spectrum was the same as that of a mixture of benzophenone and $Ni(CO)_2(PEt_3)_2$.

In kinetic studies, the rate of disappearance of $Ni(PEt_3)_3$ was followed at 500 nm. Separate solutions of $Ni(PEt_3)_4$ and benzophenones were prepared in Schlenk flasks under argon and transferred

Table VIII. Crystal and Diffractometer Data for (Benzophenone)bis(triethylphosphine)nickel

empirical formula	$NiC_{25}H_{40}OP_2$
color of crystal	dark red
space group	$P2_1/n$
cell dimens (−145 °C; 18 rflctns)	
a	11.209 (6) Å
b	19.243 (10) Å
c	11.911 (6) Å
β	96.65 (4)°
Z (molec/cell)	4
V	2551.83 Å^3
calcd density	1.242 g/cm^3
wavelength	0.710 69 Å
mol wt	477.25
linear abs coeff	8.993 cm^{-1}
detector to sample dist	22.5 cm
sample to source dist	23.5 cm
takeoff angle	2°
average ω scan width at half-height	0.27°
scan speed	3°/min
scan width	2 + dispersion
single bkgd time at extremes of scan	10 s
aperture size	3 × 3.5 mm
limits of data collecn	
min 2θ	4°
max 2θ	50°
total no. of rflctns collected	8079
no. of unique intensities	4056
no. with $F > 0.0$	3810
no. with $F > \sigma_F$	3756
no. with $F > 2.33\sigma_F$	3630
final residuals	
R_F	0.0499
R_{wF}	0.0709
goodness of fit for last cycle	1.375
max δ/σ for last cycle	0.05

by means of glass syringes to a Durrum-Gibson stopped-flow spectrophotometer. The reactions were carried out under pseudo-first-order conditions with benzophenone in excess. Reactions in hexane were followed on a Cary 14 spectrophotometer by using equimolar solutions of both reagents.

Varian T-60 and XL-100 NMR spectrometers were used to record ^1H and ^{31}P NMR spectra, and a Varian E-112 spectrometer was used for the ESR studies. Equal amounts of a 0.05 M THF solution of $Ni(PEt_3)_4$ and benzophenone were mixed and sealed in a quartz tube. Upon irradiation with a mercury lamp without any filter, a small signal appeared at −170 °C with a g value of 2.0030 and line width ~13 G. No hyperfine structure was observed. The signal disappeared when the light was turned off.

X-ray Structure Analysis. Equimolar amounts of $Ni(PEt_3)_4$ and benzophenone were mixed in a solvent consisting of a 1:10 mixture of toluene and hexane. The solution was cooled very slowly to −60 °C overnight to yield clusters of thick dark red needles. A small fragment, measuring 0.25 × 0.31 × 0.32 mm, was cleaved from a larger crystal and used for characterization and data collection. The sample was mounted on a glass fiber with silicone grease and cooled on the goniostat to −145 °C, the temperature at which all measurements were done. Because of suspected air sensitivity, the sample was mounted in a dry-nitrogen glovebag and transferred to the goniostat while bathing the crystal in dry nitrogen.

The diffractometer utilized for data collection was designed and constructed locally.[26] A Picker four-circle goniostat equipped with a Furnas monochromator (HOG crystal) and a Picker X-ray generator was interfaced to a T1980B minicomputer, with Slo-Syn stepping motors to drive the angles. Centering was accomplished by using automated top/bottom–left/right slit assemblies which are the basis of the diffractometer alignment. The minicomputer was interfaced to a CYBER172-CDC660 multimainframe system where all computations were performed.

Complete crystal and diffractometer data for the continuous θ–2θ scan technique are given in Table VIII. The data were reduced in the usual manner and the structure solved by a combination of direct methods and Patterson techniques. [All computations were made by using the IUMSC interactive XTEL program library, which consists of local code and selected programs adapted from those described by A. C. Larson (Los Alamos code) and J. A. Ibers (Northwestern University Library).] Nonhydrogen atoms thus located were refined isotropically, and a difference Fourier synthesis phased on the refined positions located all hydrogen atoms. Final full-matrix refinement using anisotropic thermal parameters for nonhydrogen atoms and isotropic thermal parameters for hydrogens converged rapidly. All data with $F > \sigma_F$ (based on counting statistics) were used in the refinement. Owing to the nearly equidimensional size of the crystal and the low linear absorption coefficient, no absorption correction was deemed necessary. An isotropic extinction parameter was included in the final refinement but did not differ significantly from zero.

The final positional and isotropic thermal parameters are given in Table IX, and observed and calculated structure factors are available (supplementary material).

Acknowledgment. We wish to thank Ms. Lydia Kelly for technical assistance, the Marshall H. Wrubel Center for the computations and the National Science Foundation for financial support.

Registry No. I, 70428-78-3; $[4\text{-}CH_3C_6H_4COC_6H_5]Ni(PEt_3)_2$, 70428-79-4; $[4\text{-}IC_6H_4COC_6H_5]Ni(PEt_3)_2$, 70428-80-7; $[4\text{-}Me_3N^+C_6H_4COC_6H_5]Ni(PEt_3)_2$, 70428-81-8; $[4\text{-}Me_2NC_6H_4\text{-}COC_6H_5]Ni(PEt_3)_2$, 70428-82-9; $Ni(PEt_3)_4$, 51320-65-1.

Supplementary Material Available: Table IX (final positional and isotropic thermal parameters) and a listing of observed and calculated structure factors (40 pages). Ordering information is given on any current masthead page. Complete crystallographic data for this compound are available, in microfiche form only, from the Indiana University Chemistry Department Library. Request IUMSC Report No. 7837 when ordering.

References and Notes

(1) (a) W. L. Driessen and W. L. Groeneveld, *Recl. Trav. Chim. Pays-Bas*, **88**, 977 (1969); **90**, 258 (1971); (b) K. Jackowski and Z. Kecki, *J. Inorg. Nucl. Chem.*, **39**, 1073 (1977).
(2) (a) W. L. Driessen and W. L. Groeneveld, *Recl. Trav. Chim. Pays-Bas*, **90**, 87 (1971), and references cited therein; (b) Compare also P. L. Verheijdt, P. H. van der Voort, W. L. Groeneveld, and W. L. Driessen, *ibid.*, **91**, 1201 (1972).
(3) W. L. Driessen, W. L. Groeneveld, and F. W. van der Wey, *Recl. Trav. Chim. Pays-Bas*, **89**, 353 (1970), and references cited therein.
(4) Metal halides also form adducts with carbonyl compounds: (a) I. Lindqvist, "Inorganic Adduct Molecules of Oxo-compounds", Springer-Verlag, New York, 1963; (b) A. Rosenheim and W. Stellmann, *Chem. Ber.*, **34**, 3377 (1901); (c) D. Cassimatis and B. P. Susz, *Helv. Chim. Acta*, **43**, 852 (1960); (d) R. C. Aggarwal and M. Onyszchuk, *J. Inorg. Nucl. Chem.*, **30**, 3351 (1968); (e) R. J. Clark, J. Lewis, D. J. Machin, and R. S. Nyholm, *J. Chem. Soc.*, 379 (1963); (f) N. N. Greenwood and P. G. Perkins, *ibid.*, 356 (1960); (g) A. F. Kapustinskii and V. A. Solokhin, *Chem. Abstr.*, **50**, 9849*e* (1956).
(5) R. Countryman and B. R. Penfold, *J. Cryst. Mol. Struct.*, **2**, 281 (1972).
(6) D. Walther, *Z. Chem.*, **15**, 490 (1975).
(7) (a) S. D. Ittel, *J. Organomet. Chem.*, **137**, 223 (1977); (b) S. D. Ittel, *Inorg. Chem.*, **16**, 2589 (1977).
(8) C. A. Tolman, W. C. Seidel, and L. W. Gosser, *J. Am. Chem. Soc.*, **96**, 53 (1974).
(9) The shift to a new absorption has not been assigned.
(10) M. Bigorgne, *J. Inorg. Nucl. Chem.*, **26**, 107 (1964).
(11) L. Nadjo and J. M. Saveant, *J. Electroanal. Chem. Interfacial Electrochem.*, **30**, 41 (1971).
(12) (a) M. J. Nilges, E. K. Barefield, R. L. Belford, and P. H. Davis, *J. Am. Chem. Soc.*, **99**, 755 (1977); (b) A. Gleizes, M. Dartiguenave, Y. Dartiguenave, J. Galy, and H. F. Klein, *ibid.*, **99**, 5187 (1977); (c) M. J. D'Aniello, Jr., and E. K. Barefield, *ibid.*, **100**, 1474 (1978).
(13) N. Hirota in "Radical-Ions", E. T. Kaiser and L. Kevan, Eds., Interscience, New York, 1968, p 35 ff.
(14) (a) A mechanism involving a rate-limiting direct displacement of phosphine from $Ni(PEt_3)_4$ is considered unlikely. (b) Furthermore, $Ni(PEt_3)_2$ derived by the second dissociation of phosphine is neglected since K is small ($<10^{-6}$ M). This assumption is supported by the fit of the rate expression in eq 9 to the phenomenological expression in eq 6.
(15) E. B. Fleisher, N. Sung, and S. Hawkinson, *J. Phys. Chem.*, **72**, 4311 (1968).
(16) (a) M. J. S. Dewar, *Bull. Soc. Chim. Fr.*, **18**, C71 (1951); (b) J. Chatt and L. A. Duncanson, *J. Chem. Soc.*, 2939 (1953).
(17) M. Aresta and C. F. Nobile, *J. Chem. Soc., Chem. Commun.*, 636 (1975).
(18) L. J. Guggenberger, *Inorg. Chem.*, **12**, 499 (1973).
(19) D. J. Yarrow, J. A. Ibers, Y. Tatsuno, and S. Otsuka, *J. Am. Chem. Soc.*, **95**, 8590 (1973).
(20) S. D. Ittel and J. A. Ibers, *Adv. Organomet. Chem.*, **14**, 33 (1976).
(21) D. J. Sepelak, C. G. Pierpont, E. K. Barefield, J. T. Budz, and C. A. Poffenberger, *J. Am. Chem. Soc.*, **98**, 6178 (1976).
(22) P. T. Cheng, C. D. Cook, C. H. Koo, S. C. Nyburg, and M. T. Shiomi, *Acta Crystallogr., Sect. B*, **27**, 1904 (1971).

(23) D. J. Brauer and C. Krüger, *J. Organomet. Chem.*, **77**, 423 (1974).
(24) J. K. Stalick and J. A. Ibers, *J. Am. Chem. Soc.*, **92**, 5333 (1970).
(25) R. A. Schunn, *Inorg. Chem.*, **15**, 208 (1976).
(26) J. C. Huffman, W. E. Streib, and C. R. Sporleder, unpublished results.

Contribution from the Departments of Chemistry, Western Washington University, Bellingham, Washington 98225, and Washington State University, Pullman, Washington 99163

Magnetic Exchange in a One-Dimensional Polymeric Chain Containing Cyanide-Bridged Copper(II)

C. P. Landee,[1a] M. Wicholas,*[1b] R. D. Willett,*[1a] and T. Wolford[1b]

Received December 8, 1978

Although cyanide rapidly reduces copper(II) to copper(I) when mixed together in aqueous solution,[2] it has recently been shown possible to isolate stable ternary copper(II) complexes containing coordinated cyanide and nitrogen donor bases.[3] This communication discusses the interaction of copper(II), 2,2′,2″-terpyridine (terpy), and cyanide, the isolation of two stable complexes [Cu(terpy)CN]NO_3·H_2O and [Cu(terpy)-CN]ClO_4, and their magnetic properties.

Magnetic interactions in these complexes should be of interest being that [Cu(terpy)CN]NO_3·H_2O is a one-dimensional polymeric chain containing cyanide, which bridges between adjacent copper(II) ions[4] whose unpaired spins should be in near-orthogonal molecular orbitals. Such chains ideally should be ferromagnetic and only one example of a one-dimensional ferromagnetic $S = {}^1/_2$ chain is presently known.[5]

Experimental section

Synthesis of [Cu(terpy)CN]X. X = ClO_4^-. A 0.100-g (4.3×10^{-4} mol) portion of terpy was dissolved with heating in a 20-mL aqueous solution containing 0.092 g (4.3×10^{-4} mol) of $Cu(NO_3)_2$·$3H_2O$. An aqueous solution (8 mL) of KCN (0.028 g, 4.3×10^{-4} mol) was added dropwise with stirring to the aforementioned hot solution, and this was followed by 5 mL of aqueous $NaClO_4$ (0.053 g, 4.3×10^{-4} mol). Blue crystals of product separated, were washed with ice-cold water, and were dried over P_2O_5 for 24 h. Anal. Calcd for [Cu-($C_{15}H_{11}N_3$)CN]ClO_4: C, 45.51; H, 2.63; N, 13.26. Found: C, 45.54; H, 2.59; N, 13.31.

X = NO_3^-. Blue crystals of the complex [Cu(terpy)CN]NO_3·H_2O were isolated as previously described.[4]

Infrared spectra were run on a Perkin-Elmer 521 and magnetic susceptibilities were determined from 1.7 to 100 K by using a PAR vibrating sample magnetometer as previously described.[6]

Results and Discussion

An initial plot of $1/\chi$ vs. T for the NO_3^- salt indicated Curie–Weiss behavior with an intercept of approximately −1 K, thus showing the presence of weak antiferromagnetic interaction. A more sensitive indication of the antiferromagnetic nature of the magnetic exchange is obtained from a plot of χT vs. T (Figure 1), as shown by the decrease of χT at low temperature. Because of the linear chain structure of the salt, the data were fit to the high-temperature series expansion of Baker et al.[7] for the $S = {}^1/_2$ Heisenberg antiferromagnet. The results of the least-squares analysis of the data are shown as the solid line in Figure 1, with $J = -0.44$ cm^{-1} and $g = 2.087$. A comparable, although somewhat poorer, fit could also be obtained from the $S = {}^1/_2$, Ising model predictions[8] with $J = -0.53$ cm^{-1} and $g = 2.105$. However, because of the nearly isotropic **g** tensor for Cu^{2+} salts, the Heisenberg model is more appropriate, and the value of $J = -0.44$ cm^{-1} is to be preferred.

In our discussion of the mechanism of superexchange responsible for $J = -0.44$ cm^{-1}, the structure of [Cu(terpy)-CN]NO_3·H_2O should first be mentioned here. Each copper(II) is in a square-pyramidal environment with the terpyridine nitrogen and cyanide carbon bonding equatorially; the apical position is occupied by a cyanide nitrogen which bridges from an adjacent Cu(terpy)CN^+ unit.[4] This is qualitatively illustrated in Figure 2.

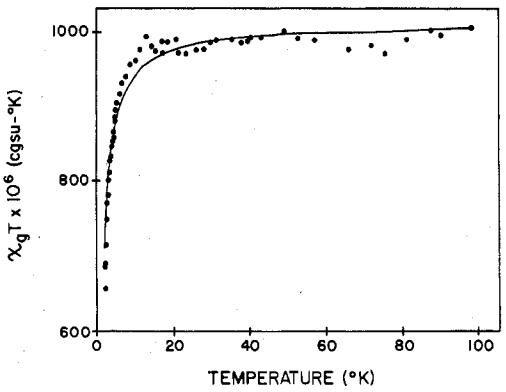

Figure 1. Plot of the function $\chi_g T$ vs. temperature for [Cu(terpy)CN]NO_3·H_2O. The dots represent the experimental values; the solid line represents the best least-squares fit.

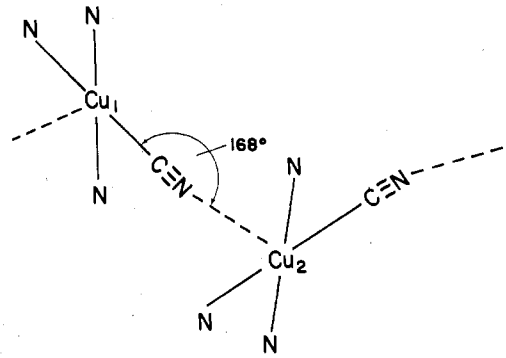

Figure 2. Geometry of the one-dimensional polymeric chain, [Cu(terpy)CN]NO_3·H_2O.

Table I. Exchange Coupling Constants and Structural Parameters for Cyanide-Bridged Copper(II)

compound[a]	J, cm^{-1}	structure[b]	cyanide bridging[c]
[Cu(terpy)CN]NO_3·H_2O	−0.44	SPY	(e,a)
[Cu_2(bpy)$_4$CN]$(PF_6)_3$[d]	−9.4	TBP	(e,e)
[Cu_2(phen)$_4$CN]$(PF_6)_3$[d]	−29	TBP	(e,e)
[Cu_2(tren)$_2$CN]$(PF_6)_3$[d]	−88	TBP	(a,a)
[Cu_2([14]4,11-diene-N_4)$_2$CN]$(ClO_4)_3$[e]	−4.8	TBP	(e,e)

[a] bpy = 2,2′-bipyridine; phen = 1,10-phenanthroline; tren = 2,2′,2″-triaminotriethylamine; [14]4,11-diene-N_4 = 5,6,6,12,14,14-hexamethyl-1,4,8,11-tetraazacyclotetradeca-4,11-diene. [b] Key: TBP = trigonal bipyramidal; SPY = square pyramidal. [c] Key: a = axial; e = equatorial; (e,a) represents (C bond, N bond). [d] Reference 9. [e] Reference 8.

The very weak antiferromagnetic coupling observed in [Cu(terpy)CN]NO_3·H_2O may be compared with the antiferromagnetic exchange interactions occurring in the four other known cyanide-bridged copper(II) complexes listed in Table I. The four complexes studied by Hendrickson[9,10] all have trigonal-bipyramidal geometry and an anticipated d_{z^2} ground state for copper(II). In each case antiferromagnetic superexchange can be rationalized by invoking overlap of d_{z^2} with σ orbitals on CN^-. For [Cu(terpy)CN]NO_3·H_2O, the anticipated ground state is $d_{x^2-y^2}$. Considering for simplicity the qualitative structure shown above, we find the $d_{x^2-y^2}$ orbital on Cu_1 has a symmetry-allowed overlap with the highest filled σ MO on cyanide. The latter however is essentially orthogonal to $d_{x^2-y^2}$ on Cu_2, and hence sizable antiferromagnetic super-

0020-1669/79/1318-2317$01.00/0